


## FIRST $\delta^{13}\text{C}$ RESULTS WITH A NEW CONNECTION BETWEEN THE EA-IRMS SYSTEM AND THE GAS INJECTION SYSTEM AT COLOGNEAMS

Martina Gwozdz<sup>1\*</sup>  • Alexander Stolz<sup>1</sup> • Andrea Jaeschke<sup>2</sup> • Stefan Heinze<sup>1</sup> • Ramona Mörchen<sup>3</sup> • Alfred Dewald<sup>1</sup> • Janet Rethemeyer<sup>2</sup> • Dennis Mücher<sup>1</sup> • Markus Schiffer<sup>1</sup>

<sup>1</sup>University of Cologne, Institute for Nuclear Physics, Zuelpicher Str. 77, Cologne, 50937, Germany

<sup>2</sup>University of Cologne, Institute for Geology and Mineralogy, Zuelpicher Str. 49b, Cologne, 50674, Germany

<sup>3</sup>Bonn University, Institute of Crop Science and Resource Conservation, Soil Science and Soil Ecology, Karlrobert-Kreiten-Strasse 13, Bonn, 53115, Germany

**ABSTRACT.** This work presents the integration of an elemental analyzer (EA) and an isotope ratio mass spectrometer (IRMS) into the 6 MV AMS system at the Institute for Nuclear Physics, University of Cologne. The AMS measurement of  $\delta^{13}\text{C}$  values for IAEA-C6 reference material resulted in  $-11.39(226)\text{‰}$ , compared to  $-10.28(32)\text{‰}$  obtained by IRMS. The EA-IRMS system was also tested with IAEA-C3, IAEA-C5, and IAEA-C7 reference materials, yielding  $-24.79(9)$ ,  $-25.18(15)$ , and  $-14.76(18)\text{‰}$  respectively. Compared to the IAEA information values given as  $-24.91(49)$ ,  $-25.49(72)$  and  $-14.48(21)\text{‰}$  respectively. To investigate an observed sample mass dependency, environmental samples from Spitzbergen were examined, showing  $\delta^{13}\text{C}$  values of  $-25.17(55)$ ,  $-25.80(31)$ , and  $-26.17\text{‰}$  in Cologne, while Hamburg recorded  $-24.8(1)$ ,  $-25.5(1)$ , and  $-26.2(13)\text{‰}$ . In summary, this new setup could enable online analysis and quasi-simultaneous measurements of  $^{14}\text{C}$ ,  $\delta^{13}\text{C}$ , and  $\delta^{15}\text{N}$  for ultra-small samples, utilizing precise  $\delta^{13}\text{C}$  values from IRMS for fractionation correction of the  $^{14}\text{C}/^{12}\text{C}$  isotopic ratio.

**KEYWORDS:** accelerator mass spectrometry, Elemental Analyser, gas injection system, IRMS.

## INTRODUCTION

At CologneAMS, it is possible to measure  $\text{CO}_2$  samples with masses as low as  $2\ \mu\text{g}$  (Melchert et al. 2018). This is achieved by oxidizing the sample within an elemental analyzer (EA) and then directing it, using the Gas Injection System (GIS), to the AMS ion source without the need for graphitization steps.

To meet the increasing demand for  $^{14}\text{C}/^{12}\text{C}$  isotopic ratio measurements of ultra-small samples ( $1\text{--}20\ \mu\text{g}$ ), improvements in isotopic fractionation correction are necessary to enhance measurement accuracy and address dating challenges in archives with low carbon content. Fractionation effects can occur during various stages of the AMS measurement, including sample preparation and oxidation, negative ionization during the sputter process, and stripping process (Hofmann et al. 1984; Arnold et al. 1989; Alderliesten et al. 1998). While AMS can directly determine  $\delta^{13}\text{C}$  values, one study suggest that values derived from IRMS exhibit greater precision, up to two orders of magnitude (Prasad et al. 2019). Furthermore McIntyre et al. (2016) investigated the International Atomic Energy Agency (IAEA) standard IAEA-C6 with an information value  $\delta^{13}\text{C}$  value of  $-10.80(47)\text{‰}$  (Rozanski et al. 1992) and demonstrated an improvement in the  $\delta^{13}\text{C}$  value from  $-12.17(224)\text{‰}$  measured by AMS to  $-10.50(2)\text{‰}$  measured by IRMS (McIntyre et al. 2016). The notation “ $12.17(224)\text{‰}$ ” indicates the value  $12.17\text{‰}$  with an associated uncertainty of  $\pm 2.24\text{‰}$ .

Motivated by these findings, a new system has been installed at CologneAMS, which combines the EA and IRMS with the existing GIS. This enables the determination of  $\delta^{13}\text{C}$  values using

\*Corresponding author. Email: [mgwozdz@ikp.uni-koeln.de](mailto:mgwozdz@ikp.uni-koeln.de)

the IRMS instead of the AMS. During sample oxidation, around 10% of the  $\text{CO}_2$  is directed to the IRMS for a  $\delta^{13}\text{C}$  measurement, while the remaining gas is directed to the GIS. From the GIS, the sample can be transferred to the HVE SO-110 B ion source, which was installed in 2015 (Stolz et al. 2017). Additionally, this setup will allow for simultaneous IRMS-AMS measurements of gaseous AMS samples from glass ampules, which are cracked within the GIS.

## MATERIALS AND METHODS

The setup consists out of four components. The first is the EA, where samples are oxidised and transferred to the second component, the IRMS. Samples are analyzed for their nitrogen and carbon content in the EA while the IRMS measures the  $\delta^{13}\text{C}$  or  $\delta^{15}\text{N}$  values. From there the sample is captured in the syringe of the GIS, where it can be led into the ion source of the AMS.

### EA and IRMS

For combustion, all solid samples are placed in cleaned tin boats and then oxidized in the EA. The used device is a *vario isotope select* which is sold by Elementar, Germany (serial no.15191004). By introducing  $\text{O}_2$  into the combustion reactor of the EA, the sample undergoes oxidation and becomes gaseous. Helium is used as a carrier gas to transport the sample throughout the system. Within the reduction tube, the  $\text{NO}$  and  $\text{NO}_2$  gas are reduced to  $\text{N}_2$ , while other combustion products are filtered out.

After exiting the reduction tube, the gas is separated using thermal programmed desorption (TPD).  $\text{CO}_2$  is captured at approximately  $38^\circ\text{C}$ , while the nitrogen gas reaches the thermal conductivity detector (TCD) of the EA. The TCD signal provides a peak area indicating the concentration of the incoming gas components. The TCD peak areas are calibrated using reference material. The reference material has a known elemental content which is used to calibrate the measured peak areas of the carbon and nitrogen peaks. Once the nitrogen gas passed through, the TPD unit is heated to  $210^\circ\text{C}$ , causing the release of  $\text{CO}_2$ , which is then detected by the TCD.

The isoprime precisION IRMS (by Elementar) comprises an ion source that generates positive ions, an electromagnet for momentum separation, and an electrostatic analyzer (ESA). The nitrogen and carbon gases reach the ion source of the IRMS, where they undergo ionization through electron interaction. The positive ions are directed into the electromagnet, and masses 44, 45, and 46 for  $\text{CO}_2$  and 28, 29, and 30 for  $\text{N}_2$  are separated. They are individually detected in three Faraday cups.

### Gas Injection System

The GIS is a well-established component of the setup at CologneAMS. Its purpose is to capture  $\text{CO}_2$  gas from the EA using a zeolite trap and subsequently release it into a syringe. Inside the syringe, the  $\text{CO}_2$  gas is mixed with helium before being transferred to the AMS ion source. The zeolite trap used in this setup has a capacity of up to  $1000\ \mu\text{g}$  of carbon. Further details of the GIS can be found in Stolz et al. (2019, 2020) and Wacker et al. (2013).

### Connection between EA-IRMS and AMS

This section provides an overview of the newly installed hardware and software connections that link the EA, IRMS, and AMS systems. There are two possibilities to connect these

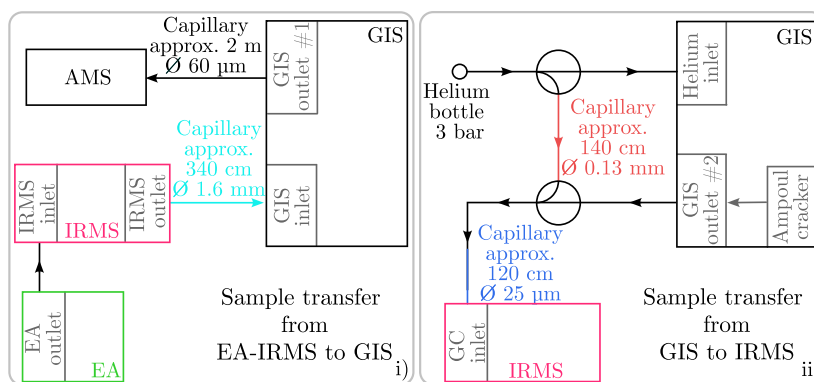


Figure 1 The schematic diagram illustrates the connection between the EA, IRMS, GIS, and AMS systems. In i), the connection is established for a sample which is oxidized in the EA. Subsequently, the gaseous sample is transferred through a capillary to a T-piece. Around 10 percent of the sample is directed towards the IRMS through a capillary (cyan) for measurement, while the remaining portion is further transferred to the GIS for subsequent analysis in the AMS ion source. Figure 1 ii) depicts the setup for pre-existing gaseous samples that can be cracked within the ampoule cracker of the GIS. The cracked sample is then transferred to the IRMS under a continuous flow of helium. This is accomplished by splitting an existing capillary, which supplies helium to the GIS, using a T-piece and an additional capillary (red).

systems. Figure 1 illustrates the general layout of the two setups. In Figure 1 i), the connection is shown, where samples are oxidized in the EA and a percentage of the gas is transferred to the IRMS, while capturing the rest in the GIS. Figure 1 ii) shows the pathway for sample gas which was cracked and then captured in the syringe of the GIS. A portion of the gas can be led to the IRMS, while retaining the remainder for a measurement with the AMS.

For the software connection the EA and the IRMS can be controlled via an application programming interface (API). The API sends out the requests to start or stop a measurement and also collects the incoming data from the various components. The API allows the gas injection control software (GICS) (Stolz et al. 2020) to communicate with the IRMS, this way the GICS software can fully control the measurement.

For samples combusted in the EA, the EA and IRMS are connected via 1/16-inch diameter tubing. The oxidized sample is transferred through this tubing. A T-piece creates a split, and an additional capillary with a 0.005-inch inner diameter is attached, leading to the IRMS inlet. This setup allows approximately 10% of the sample to enter the IRMS inlet for IRMS measurement, while the remaining portion is directed to the GIS. This is visualized in Figure 1 i). From the EA inlet, the sample gas flows towards a cold zeolite trap, where CO<sub>2</sub> is captured. Once all the CO<sub>2</sub> is inside the zeolite trap, it is heated to 450°C, allowing the CO<sub>2</sub> gas to diffuse into the syringe.

To enable the measurement of pre-existing gaseous samples, an additional connection has been established between the GIS and the IRMS. In future applications, CO<sub>2</sub> samples in glass ampoules will be cracked using the GIS ampoule cracker, and the resulting gas is transferred to the syringe. A small percentage of the sample gas can be directed into the IRMS, while the remaining gas is retained in the syringe for analysis using the AMS setup. Continuous helium flow is necessary for the operation of the IRMS ion source as the carrier gas for CO<sub>2</sub>, as depicted in Figure 1 ii). The capillary responsible for conveying CO<sub>2</sub> from the GIS to the IRMS

Table 1 The measured  $\delta^{13}\text{C}$  values, along with their corresponding standard deviations, are compared to the information value values provided by the IAEA. The IAEA information values are denoted as  $\delta^{13}\text{C}_{\text{PDB}}$ , representing their expression relative to Pee Dee belemnite (PDB). The data obtained in this work is presented as  $\delta^{13}\text{C}_{\text{Cologne}}$ .

Standard	IAEA-C3	IAEA-C5	IAEA-C7
$\delta^{13}\text{C}_{\text{PDB}}$ [‰]	-24.91(49)	-25.49(72)	-14.48(21)
$\delta^{13}\text{C}_{\text{Cologne}}$ [‰]	-24.79(9)	-25.18(15)	-14.76(18)
Number of samples	31	72	72

is equipped with a T-piece, through which helium is introduced. To achieve a low helium flow, a capillary (red) with a 0.005-inch inner diameter is connected via a T-piece to the main helium line, which also supplies the GIS.

The introduction of  $\text{CO}_2$  into the IRMS is accomplished using an open split. The GIS includes a GIS outlet #2 with a tubing of 1/16-inch diameter, which is inserted into the GC capillary of the IRMS. A piece of plastic is placed around the open split and heated. As the plastic shrinks, it secures both capillaries in place.

## RESULTS AND DISCUSSION

### EA and IRMS

This section provides an overview of the measurements conducted on different standard materials and environmental samples using the EA and the IRMS. It should be noted that the EA-IRMS setup was not connected to the GIS or AMS for these measurements.

#### *IRMS Standard Samples*

Various standard materials were oxidized in the EA, and their  $\delta^{13}\text{C}$  values were determined using the IRMS (see Table 1). The initial tests utilized the following reference material from the IAEA: IAEA-C3, IAEA-C 5, IAEA-C6, as well as IAEA-C7 and IAEA-C8. The  $\delta^{13}\text{C}$  information values of these reference materials are provided relative to the Pee Dee belemnite scale (IAEA 2014).

Over a three-month period, samples of each standard weighing between 0.030 mg and 2.000 mg were analyzed. This extensive range of sample sizes was chosen to thoroughly evaluate the oxidation process in the EA and the results of the IRMS. Each set of reference material underwent at least two measurement sequences, and no reactor changes were made throughout the analysis.

Figure 2 i) presents the results of the measured  $\delta^{13}\text{C}$  values for the reference materials IAEA-C3, IAEA-C5, and IAEA-C7, calibrated using IAEA-C6 and IAEA-C8 as reference material. Notably, it was observed that samples with masses exceeding 1.300 mg led to current saturation in the IRMS Faraday cups. Consequently, the application is limited to samples weighing up to 1.300 mg.

The results, depicted in Figure 2, indicate a mass dependency in the  $\delta^{13}\text{C}$  values of all three reference materials. To address this issue, a linear fit was applied to the data, resulting in the following fit equations: IAEA-C3:  $y_{c3}(x) = 0.4298 \cdot x - 0.1232$ , IAEA-C5:  $y_{c5}(x) = 0.4020 \cdot x + 0.0720$ , and IAEA-C7:  $y_{c7}(x) = 0.1247 \cdot x - 0.3494$ . To correct for this mass dependency,

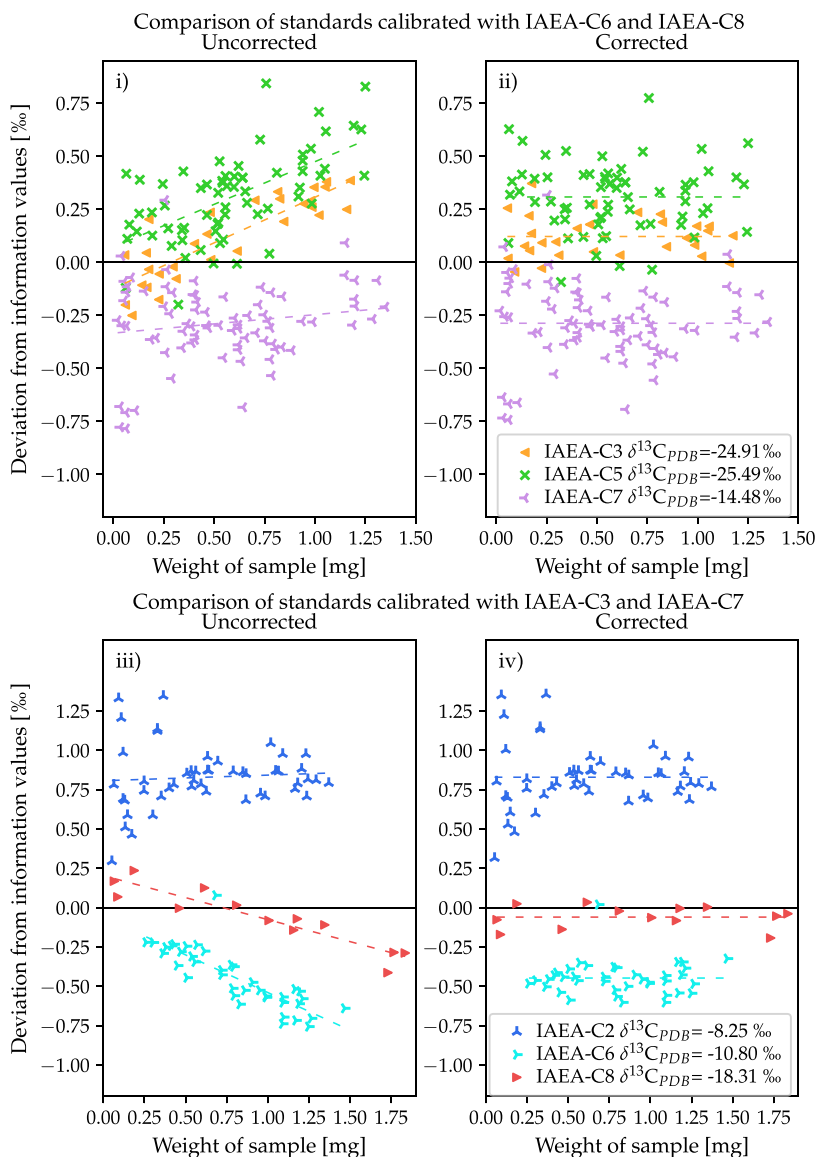


Figure 2 i), the  $\delta^{13}\text{C}$  values of IAEA-C3, IAEA-C5, and IAEA-C7 are presented as initially calculated. These data points exhibit a mass dependency, which is addressed by applying a linear fit (shown as a dotted line) for correction. In Figure 2 ii), the corrected data is displayed. The data is calibrated to the  $\delta^{13}\text{C}_{\text{PDB}}$  scale, utilizing measurements from IAEA-C6 and IAEA-C8. Figures iii) and iv) show the same plot but with reference materials IAEA-C2, IAEA-C6 and IAEA-C8, which are calibrated with IAEA-C3 and IAEA-C7.

the  $\delta^{13}\text{C}$  values are transformed in a way that after transformation the linear fit of the data results in a slope of zero. The corrected values are illustrated in Figure 2 ii). Table 1 shows the standard deviations of the corrected  $\delta^{13}\text{C}$  values.

This mass dependency was also seen for a similar set of measurements of three additional reference materials. The mass dependency in Figure 2 could be interpreted as a dependency to

Table 2 The measured  $\delta^{13}\text{C}$  values and carbon content of the environmental samples from Spitzbergen, along with their corresponding standard deviations, are presented. The  $\delta^{13}\text{C}_{\text{HH}}$  values represent the measurements conducted in Hamburg, while the data obtained in this study are provided as  $\delta^{13}\text{C}_{\text{Cologne}}$ .

Sample	COL5119	COL5115	COL5111
$\delta^{13}\text{C}_{\text{HH}}$ [‰]	-24.8(1)	-25.5(1)	-26.2(13)
$\delta^{13}\text{C}_{\text{Cologne}}$ [‰]	-25.17(55)	-25.80(31)	-26.17(77)
Carbon content [%]	1.3(14)	1.62(67)	2.9(12)
# of samples measured (Cologne)	35	23	23

the carbon content, with a lower  $\delta^{13}\text{C}$  value the slope becomes less steep. However, this effect could not be confirmed with the additionally measured reference materials which can be seen in Figure 2 iii) and iv).

Comparing the  $\delta^{13}\text{C}$  values of the IAEA reference materials with those measured at Cologne, it is found that they fall within the expected range, with statistical uncertainties below 0.2‰. This demonstrates a good and reproducible agreement with the IAEA information values. Additionally, it is worth mentioning that the careful selection of calibration reference materials is crucial. In this study, two reference materials were chosen, to provide a large  $\delta^{13}\text{C}$  calibration range. As can be seen in Figure 2 this can lead to deviations from the information values. Therefore, for a more precise calibration technique, Coplen et al. (2006) can be utilized.

#### *Samples from Spitzbergen, Norway*

In addition, environmental samples COL5115, COL5111, and COL5119 collected from Spitzbergen, Norway, were analyzed for their  $\delta^{13}\text{C}$  values. These samples had previously been measured at the Institute of Soil Science, University of Hamburg, and are labeled as  $\delta^{13}\text{C}_{\text{HH}}$ . Prior to analysis, the environmental samples underwent decalcification using phosphoric acid, following the method described by Rethemeyer et al. (2019). The  $\delta^{13}\text{C}$  values were measured using a Delta V instrument (Thermo Scientific) (Knoblauch et al. 2013). Each environmental sample was measured twice by the Institute of Soil Science and the given uncertainties is the standard deviation between those two points. Detailed  $\delta^{13}\text{C}$  values and their corresponding uncertainties are provided in Table 2.

A total of 81 samples were analyzed, ranging in sample masses from 0.060 to 1.300 mg. The samples underwent oxidation in the EA using a helium flow rate of 250 ml/min, and their  $\delta^{13}\text{C}$  values were determined in the IRMS using IAEA-C3 and IAEA-C6 for calibration. It is worth noting that the  $\delta^{13}\text{C}$  values of the COL samples are similar to each other, indicating that the calibration procedure using only two reference materials was sufficient for all three samples. However, it is important to exercise caution when calibrating the IRMS system for samples with significantly different  $\delta^{13}\text{C}$  values to ensure accurate results within each range.

Furthermore, the carbon contents of the samples were determined using the EA and are listed in Table 2. Unlike the reference materials, only the environmental sample COL5115 exhibited a noticeable mass dependency, which was subsequently corrected for. This correction is illustrated in Figure 3.

The  $\delta^{13}\text{C}$  values of the COL samples have a larger standard deviation of up to 0.77‰ compared to those of the standard material with 0.18‰ for IAEA-C7. The reason for the larger scattering

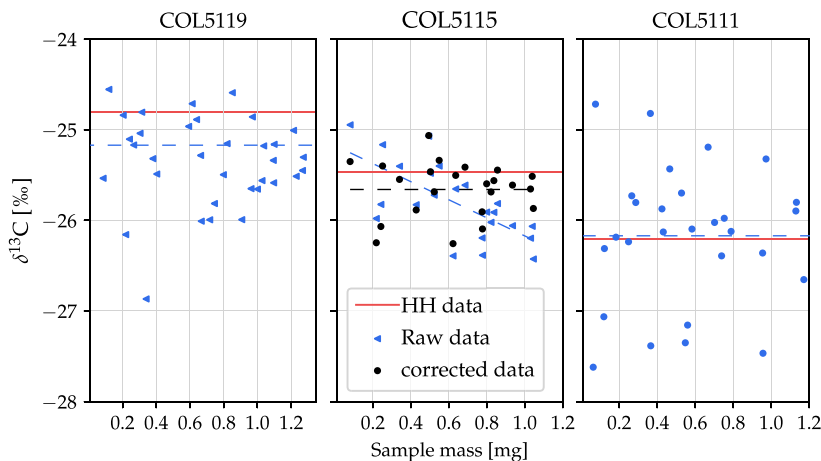


Figure 3 The  $\delta^{13}\text{C}$  values of three environmental samples collected from Spitzbergen and measured at CologneAMS are presented in blue with their average value. These values are compared to measurements from Hamburg, represented by the red line. Furthermore, the  $\delta^{13}\text{C}$  values have been corrected for their mass dependency, and the corrected data is depicted in black.

can on the one hand be the characteristic of soil samples. On the other hand the standard deviations of the samples in this work result in a statistically significant value, due to the large number of samples, compared to the two measurements per sample done in Hamburg.

Additionally, it is important to acknowledge that the mass dependency effect is not yet fully understood and requires further investigation. To minimize potential uncertainties associated with the mass dependency, future measurements will employ samples and reference materials with similar  $\delta^{13}\text{C}$  values and masses.

#### $\delta^{15}\text{N}$ values for Atacama Samples

Environmental samples from the Atacama desert in Chile were analyzed for their  $\delta^{15}\text{N}$  values and compared to measurements conducted at the University of Bonn using an already established EA-IRMS system. The system in Bonn utilizes a Thermo Fisher Scientific Flash EA 1112 series, which is connected to a Conflo III interface and a Delta V Advantage IRMS.

For the analysis, the samples were weighed at approximately 200 mg in both institutes and measured alongside IAEA-N1 ( $\delta^{15}\text{N} = +0.43\text{‰}$ ) and IAEA-N2 ( $\delta^{15}\text{N} = +20.41\text{‰}$ ) reference materials to calibrate the  $\delta^{15}\text{N}$  values. The environmental samples exhibit very low nitrogen content, averaging at 0.03 percent. Due to the low nitrogen content, larger sample sizes were required compared to standard carbon samples.

The first test series in Cologne was conducted on three different days of two weeks, during which the EA reactors remained unchanged. The samples were measured in ascending order based on their names. Each data point represents the average of approximately three samples of the same sample material. A more detailed listing can be found in Table 3. Figure 4 i) presents a comparison of the  $\delta^{15}\text{N}$  values obtained in Cologne and Bonn. The data indicates a discrepancy towards lower  $\delta^{15}\text{N}$  values for the samples measured last (Loa10, Loa11, Loa12). Further investigation revealed that these samples were only partially oxidized, likely accounting for the observed differences in  $\delta^{15}\text{N}$  values.

Table 3  $\delta^{15}\text{N}$  along with their corresponding standard deviations of environmental samples from the Atacama desert measured with the EA-IRMS system at CologneAMS.

Sample	# of samples	$\delta^{15}\text{N}$ [‰]	# of samples	$\delta^{15}\text{N}$ [‰]
Loa1	3	5.07(27)	2	5.22(40)
Loa2	4	5.72(23)	1	4.15
Loa3	4	4.22(112)	1	4.40
Loa4	2	2.66(255)	1	-1.50
Loa5	3	1.78(61)	1	1.36
Loa6	3	-0.09(63)	2	0.92(490)
Loa7	3	1.12(112)	1	6.90
Loa8	3	-0.28(65)	2	-0.8(100)
Loa9	2	2.32(25)	1	3.64
Loa10	3	-0.34(119)	2	4.04
Loa11	3	1.07(131)	2	3.86(250)
Loa12	3	1.04(21)	2	-3.88(575)

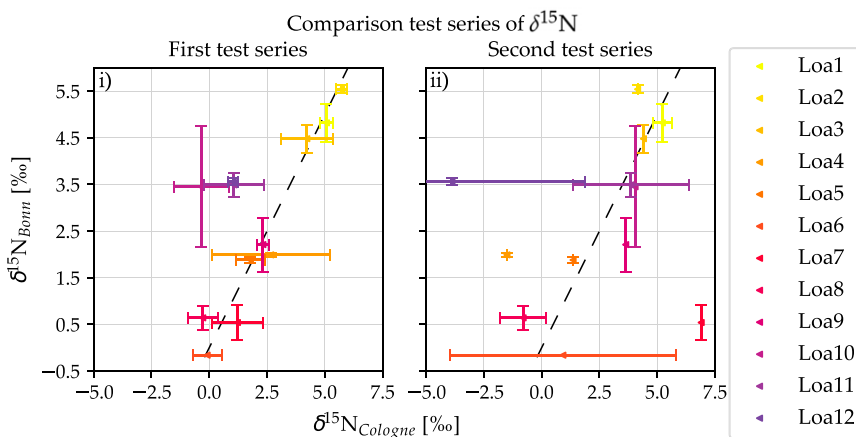


Figure 4 The two test series of the Atacama environmental samples are shown. The first test series, i) were measured in ascending order of the samples names. The second test series, ii), the samples were measured in descending order and with an extended  $\text{O}_2$  window during the combustion in the EA. This is done to ensure the full combustion of the samples. The errorbars show the standard deviation of the individual set of samples. If the data point does not have an errorbar, only one sample was measured. The identity line is depicted as a dotted line in the figures, serving as a reference.

To test this hypothesis, a second series was conducted in reverse order, starting with the Loa12 sample and proceeding in descending order of the sample names. This second test series is depicted in Figure 4 ii). The samples were measured on two different days without changing the reactors, and the  $\text{O}_2$  window for combustion was extended from 80 s to 100 s. Due to limited sample material, most of the samples in the second test series could only be measured once or twice.

The  $\delta^{15}\text{N}$  values in the second series exhibit greater scattering compared to the first series, likely due to the low number of measured samples and the heterogeneous nature of the soils. Additionally, it can be observed that the scattering no longer depends on the order in which the samples were measured, indicating that the deviation is now independent of sample order.



Excluding the sample Loa10, Loa11 and Loa12, the results of the first test series demonstrate that this setup is capable of reliably measuring  $\delta^{15}\text{N}$  values from environmental samples, and the results are comparable to those from other institutes. However, results for Loa10–Loa12 emphasize on a careful execution of the combustion, to ensure that unknown or large sample are fully oxidized.

The standard deviations of the sample material, in comparison to the reference materials, show an increase. While the standard deviation of the IAEA-N2 reference materials is 0.08‰, the samples exhibit standard deviations of up to 2.5‰. This difference may be attributed to the non-homogeneous nature of the samples and warrants further investigation with a larger sample size. The effect could also stem from an incomplete reduction of  $\text{NO}_x$  to  $\text{N}_2$ , but the chromatograms of  $m/z$  28 did not show any abnormalities. Overall, Figure 4 i) illustrates that the  $\delta^{15}\text{N}$  values obtained from the new setup largely exhibit good consistency with the results from Bonn University.

### Connection

In this section the two setups shown in Figure 1 are tested with standard material.

#### *GIS to IRMS*

The connection between the GIS and the IRMS was assessed by introducing varying masses of Ox-II gas into the system. The Ox-II gas is a mixture consisting of 5 percent Ox-II and the remaining portion being helium. The carbon mass was determined by measuring the pressure within a known volume of syringe, tubes, and fittings (Stolz et al. 2020). The bottled Ox-II gas was directly transferred to the syringe of the GIS. Target carbon sample masses of 0.495(3)  $\mu\text{g}$ , 0.745(1)  $\mu\text{g}$ , 0.981(17)  $\mu\text{g}$ , 1.896(7)  $\mu\text{g}$ , 2.888(9)  $\mu\text{g}$ , 3.922(9)  $\mu\text{g}$ , 4.628(7)  $\mu\text{g}$ , 5.942(5)  $\mu\text{g}$ , 6.610(202)  $\mu\text{g}$ , and 7.714(2)  $\mu\text{g}$  were transferred from the GIS syringe to the IRMS. Four measurements were conducted for each mass, and the average  $\delta^{13}\text{C}$  value was plotted against the mass in Figure 5. The  $\delta^{13}\text{C}$  measurements were calibrated using the 7.71  $\mu\text{g}$  Ox-II sample.

The test of the connected GIS and IRMS system, shown in Figure 5, yielded reliable  $\delta^{13}\text{C}$  values, except for carbon masses below 2  $\mu\text{g}$ , where the  $\delta^{13}\text{C}$  values exhibited scattering. While the  $\delta^{13}\text{C}$  value for 6.610  $\mu\text{g}$  could stem from the larger mass scattering of  $\pm 0.202$   $\mu\text{g}$  the  $\delta^{13}\text{C}$  value for 4.628  $\mu\text{g}$  cannot be explained by this. Nonetheless the  $\delta^{13}\text{C}$  value is still within the range of the information value.

The data points above 2  $\mu\text{g}$  exhibit a standard deviation of the  $\delta^{13}\text{C}$  values ranging from 0.03 to 0.06‰, except for the 4.63  $\mu\text{g}$  and 6.61  $\mu\text{g}$  samples which have standard deviations of 0.19‰ and 0.16‰, respectively.

For sample masses below 2  $\mu\text{g}$ , deviations from the information value become more significant, potentially due to constant contamination. In this setup, the deviation from the information value can reach up to  $\pm 0.6$ ‰. Although the standard deviation for the 0.49  $\mu\text{g}$  and 0.75  $\mu\text{g}$  samples is  $\pm 0.2$ ‰, this would still result in reliable  $\delta^{13}\text{C}$  measurements, if the calibration gas volume is kept the same as the sample gas, but it could result in larger uncertainties.

Further testing of this setup is necessary to determine if the deviations from the information value are caused by constant contamination. The data collected thus far is not sufficient to draw definitive conclusions.

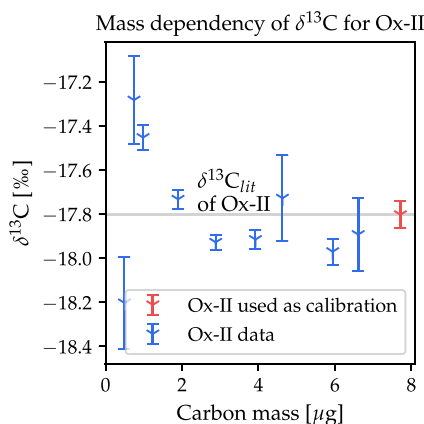


Figure 5 The graphic shows the test series for the connected GIS-IRMS system. Different sample sizes of Ox-II are transferred into the IRMS and its  $\delta^{13}\text{C}$  value is measured. The data is calibrated using the 8  $\mu\text{g}$  sample. The errorbars show the standard deviation of the set of one sample mass.

Additionally, as depicted in the Chapter *IRMS Standard Samples*, the  $\delta^{13}\text{C}$  values of solid samples analyzed using the EA-IRMS display a dependency on sample mass. In contrast, the gaseous samples discussed in this chapter do not exhibit such a dependency. It is important to highlight that the sample masses measured in both setups are comparable, as indicated by the similar peak areas measured with the IRMS. This observation suggests that this effect could stem from either the sample or the EA system itself. Further investigation needs to be conducted to find the cause of the mass dependency.

#### EA-IRMS to GIS

This section presents the first results of the combustion of samples in the EA and the quasi-simultaneous measurement of  $\delta^{13}\text{C}$  with the IRMS and AMS.

In the first test measurement, 32 IAEA-C6 samples with a  $\delta^{13}\text{C}$  value of  $-10.8\text{‰}$  were measured using the setup shown in Figure 1 i). Alongside, eight Ox-II samples and two blank samples were also measured for calibration. All samples had a carbon mass of around 100  $\mu\text{g}$ .

The IAEA-C6  $\delta^{13}\text{C}$  obtained from the AMS measurements was corrected using the blank and Ox-II samples, while the IAEA-C6 data from the IRMS measurements was calibrated and corrected using the data from the Ox-II samples and two empty tin boats that were measured as well. The evaluated data is presented in Figure 6.

Figure 6 shows that the AMS measurements of the  $\delta^{13}\text{C}$  have a standard deviation seven times larger than the IRMS data. Additionally, the  $\delta^{13}\text{C}$  values obtained from the AMS measurements fall within the standard deviation of the IAEA-C6 measured using IRMS. This is similar to McIntyre et al. (2016), where the IRMS  $\delta^{13}\text{C}$  value lies within the given standard deviation.

Reasons for the more precise  $\delta^{13}\text{C}$  could lie within the different ion sources that are used in the AMS and IRMS. But the results presented in this work lie close to another and could give rise to the possibility to use the  $\delta^{13}\text{C}$  from the IRMS for the fractionation correction. In the future further test will be conducted to find if the  $\delta^{13}\text{C}$  from the AMS could have a systematical offset compared to the IRMS  $\delta^{13}\text{C}$  data.

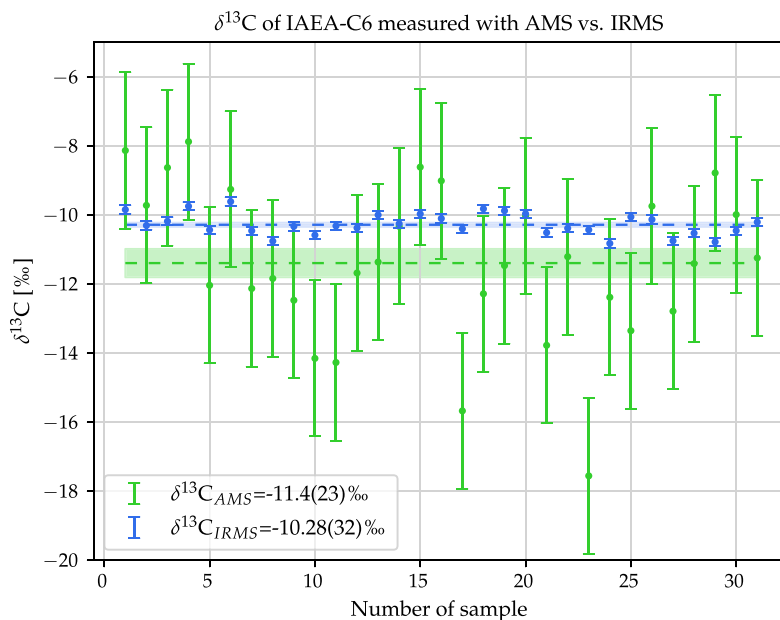


Figure 6 Shown are the  $\delta^{13}\text{C}$  values of IAEA-C6 which has an information value of  $\delta^{13}\text{C}_{\text{PDB}} = -10.80(47)\text{‰}$ . The blue data represents the values measured by the IRMS, while the green is the data measured by the AMS. The dotted lines show the average values respectively and the filled in area is the uncertainties of the average. The error bars show the standard deviation of the complete set of either AMS or IRMS measured samples.

## CONCLUSION

The 6 MV AMS system at the University of Cologne, which is used for routine  $^{14}\text{CO}_2$  measurements, has been expanded with the integration of an EA-IRMS system, to enable the quasi-simultaneous measurement of  $\delta^{13}\text{C}$ . The entire system is now computer-controlled using a single software.

While the mass dependency found in Chapter *IRMS Standard Samples* needs to be further investigated to find its origin, standard materials and environmental samples consistently yield reproducible  $\delta^{13}\text{C}$  values that are comparable to the results reported by Knoblauch et al. (2013). Additionally, a good agreement was observed between the  $\delta^{15}\text{N}$  values of Atacama environmental samples measured using the new EA-IRMS system and those obtained from the established EA-IRMS system at Bonn University.

Furthermore, our tests demonstrate that the new EA-IRMS-GIS system allows for the transfer of gaseous samples from the GIS to the IRMS. While this setup is still in progress and requires further testing, the initial measurements of  $\delta^{13}\text{C}$  values have been reliably obtained with sample masses as low as  $2\ \mu\text{g}$ . However, the measurement of  $\delta^{13}\text{C}$  of samples below  $2\ \mu\text{g}$  need to be treated with caution.

As an initial step, the  $\delta^{13}\text{C}$  of IAEA-C6 standard material was successfully measured using both the IRMS and AMS. This system enables precise measurements of a small amount of sample gas for  $\delta^{13}\text{C}$  values while the rest is transferred to the AMS system. Eventually, this development could enable the use of IRMS  $\delta^{13}\text{C}$  values to correct for fractionation in AMS measurements.

## ACKNOWLEDGMENTS

The research is supported by the CRC1211. We thank Christian Knoblauch and Ramona Mörchen for their supply of the EA-IRMS data.

## REFERENCES

- Alderliesten C, Van Der Borg K, De Jong AFM. 1998. Contamination and fractionation effects in AMS-measured  $^{14}\text{C}/^{12}\text{C}$  and  $^{13}\text{C}/^{12}\text{C}$  ratios of small samples. *Radiocarbon* 40(1), 215–221. doi: [10.1017/S0033822200018075](https://doi.org/10.1017/S0033822200018075)
- Arnold M, Bard E, Maurice P, Valladas H, Duplessy JC. 1989.  $^{14}\text{C}$  dating with the Gif-sur-Yvette Tandem accelerator: status report and study of isotopic fractionation in the sputter ion source. *Radiocarbon* 31(3), 284–291. doi: [10.1017/s0033822200011814](https://doi.org/10.1017/s0033822200011814)
- Coplen TB, Brand WA, Gehre M, Groening M, Meijer HAJ, Toman B, Verkouteren RM. 2006. New Guidelines for  $\delta^{13}\text{C}$  Measurements. *Analytical Chemistry* 78(7), 2439–2441. doi: [10.1021/ac052027c](https://doi.org/10.1021/ac052027c)
- Hofmann H, Bonani G, Morenzoni E, Nessi M, Suter M, Woelfli W. 1984. Charge state distributions and resulting isotopic fractionation effects of carbon and chlorine in the 1–7 MeV energy range. *Nuclear Instruments and Methods in Physics Research B: Beam Interactions with Materials and Atoms* 5(2), 254–258. doi: [10.1016/0168-583X\(84\)90522-6](https://doi.org/10.1016/0168-583X(84)90522-6)
- IAEA (International Atomic Energy Agency Department of Nuclear Sciences and Applications IAEA Environment Laboratories). 2014. Reference sheet for quality control material. <https://nucleus.iaea.org/sites/ReferenceMaterials/Shared>
- Knoblauch C, Beer C, Sosnin A, Wagner D, Pfeiffer EM. 2013. Predicting long-term carbon mineralization and trace gas production from thawing permafrost of northeast Siberia. *Glob. Change Biology* 19, 1160–1172. doi: [10.1111/gcb.12116](https://doi.org/10.1111/gcb.12116)
- McIntyre CP, Wacker L, Haghpor N, Blattmann TM, Fahrni S, Usman M, Eglinton TI, Synal HA. 2016. Online  $^{13}\text{C}$  and  $^{14}\text{C}$  gas measurements by EA-IRMS-AMS at ETH Zuerich. *Radiocarbon* 59(3), 893–903. doi: [10.1017/rdc.2016.68](https://doi.org/10.1017/rdc.2016.68)
- Melchert JO, Stolz A, Dewald A, Gierga M, Wischhoefer P, Rethemeyer J. 2018. Exploring sample size limits of AMS gas ion source  $^{14}\text{C}$  analysis at CologneAMS. *Radiocarbon* 61(6), 1785–1793. doi: [10.1017/RDC.2019.143](https://doi.org/10.1017/RDC.2019.143)
- Prasad GVR, Culp R, Cherkinsky A. 2019.  $^{13}\text{C}$  correction to AMS data: Values derived from AMS vs IRMS values. *Nuclear Instruments and Methods in Physics Research Section B: Beam Interactions with Materials and Atoms* 455, 244–249. doi: [10.1016/j.nimb.2019.01.034](https://doi.org/10.1016/j.nimb.2019.01.034)
- Rethemeyer J, Gierga M, Heinze S, Stolz A, Wotte A, Wischhoefer P, Berg S, Melchert JO, Dewald A. 2019. Current sample preparation and analytical capabilities of the radiocarbon laboratory at CologneAMS. *Radiocarbon* 61(5), 1449–1460. doi: [10.1017/RDC.2019.16](https://doi.org/10.1017/RDC.2019.16)
- Rozanski K, Stichler W, Gonfiantini R, Scott EM, Beukens RP, Kromer B, van de Plicht J. 1992. The IAEA  $^{14}\text{C}$  Intercomparison Exercise 1990. *Radiocarbon* 34(3), 506–519. doi: [10.1017/S0033822200063761](https://doi.org/10.1017/S0033822200063761)
- Stolz A. 2020. Einrichtung und Weiterentwicklung eines  $^{14}\text{CO}_2$  Systems am 6 MV TANDETRON Beschleuniger des CologneAMS [dissertation].
- Stolz A, Dewald A, Altenkirch R, Herb S, Heinze S, Schiffer M, Feuerstein C, Mueller-Gatermann C, Wotte A, Rethemeyer J, Dunai TJ. 2017. Radiocarbon measurements of small gaseous samples at CologneAMS. *Nuclear Instruments and Methods in Physics Research, Section B: Beam Interactions with Materials and Atoms* 406(A), 283–286. doi: [10.1016/j.nimb.2017.03.031](https://doi.org/10.1016/j.nimb.2017.03.031)
- Stolz A, Dewald A, Heinze S, Altenkirch R, Hackenberg G, Herb S, Mueller-Gatermann C, Schiffer M, Zitzer G, Wotte A, Rethemeyer J, Dunai TJ. 2019. Improvements in the measurement of small  $^{14}\text{CO}_2$  samples at CologneAMS. *Nuclear Instruments and Methods in Physics Research, Section B: Beam Interactions with Materials and Atoms* 439, 70–75. doi: [10.1016/j.nimb.2018.12.008](https://doi.org/10.1016/j.nimb.2018.12.008)
- Wacker L, Fahrni SM, Hajdas I, Molnar M, Synal HA, Szidat S, Zhang YL. 2013. A versatile gas interface for routine radiocarbon analysis with a gas ion source. *Nuclear Instruments and Methods in Physics Research B: Beam Interactions with Materials and Atoms* 294, 315–319. doi: [10.1016/j.nimb.2012.02.009](https://doi.org/10.1016/j.nimb.2012.02.009)